Sensors and Materials, Vol. 31, No. 6 (2019) 1831–1845
MYU Tokyo

S & M 1902

Enhancing Validity of Green Building Information Modeling with Artificial-neural-network-supervised Learning —Taking Construction of Adaptive Building Envelope Based on Daylight Simulation as an Example

Shang-Yuan Chen*

School of Architecture, Feng Chia University, No. 100, Wenhwa Rd., Seatwen, Taichung, Taiwan 40724, R.O.C.

(Received October 1, 2018; accepted February 12, 2019)

Keywords: Green BIM, neural-network-supervised learning, CNS illuminance standard

Green building information modeling (Green BIM) is focused on a project using BIM as a basic tool from the beginning of the design stage and employs building performance analysis (BPA) in the design-analysis decision-making cycle to obtain an optimized design proposal. However, there are inevitable discrepancies between the simulated performance data and the data obtained from the actual environment. Neural network learning can be used in conjunction with training to obtain a predictive ability, and the resulting predictive values are more representative of actual performance than simulation values. In this study, it is proposed that a predictive value be used instead of a simulation value in judging whether design goals have been met. To construct an adaptive building envelope based on daylight simulation, this project plans to carry out the following six steps in a two-stage process: Stage 1: Data collection and learning: (1) BIM modeling, (2) BPA performance simulation, (3) production of an actual structure and illuminance measurement, and (4) collection of sample data to perform training in supervised neural network learning. Stage 2: After obtaining a predictive ability: (5) setting targets to find an optimized adaptation plan and (6) implementation of script-oriented automatic control.

1. Introduction

Integrated design and analysis procedures based on green building information modeling (Green BIM) have become an important tool for architects and design teams wishing to select and improve design proposals. Nevertheless, when using building performance analysis (BPA) software to predict building performance in actual environments, there are inevitable discrepancies σ_s between simulation data obtained from the software and measurements in the actual environment (Fig. 1), which have caused the validity of the software's simulation performance to be questioned. The project discussed in this paper therefore seeks to use supervised learning by a neural network to reduce this gap and enhance the optimization ability of Green BIM.

*Corresponding author: e-mail: shangyuanc@gmail.com
https://doi.org/10.18494/SAM.2019.2147

ISSN 0914-4935

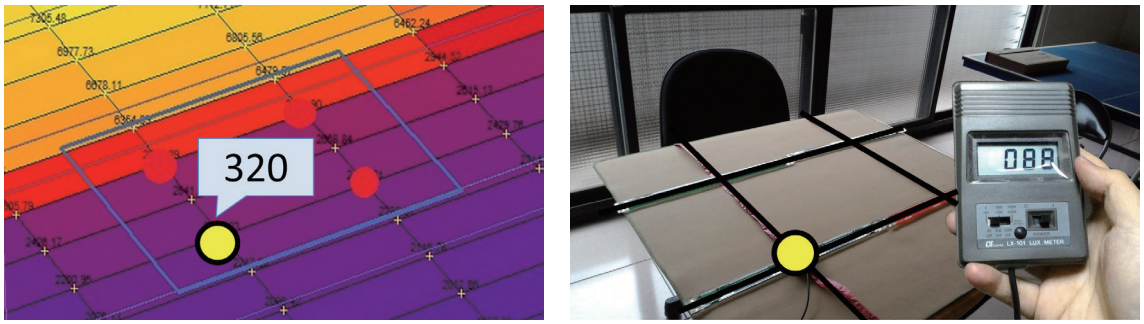

(a) (b)

Fig. 1. (Color online) Discrepancies consistently exist between (a) performance simulation data and (b) actual measurement data.

2. Literature Review

This study addresses the subjects of Green BIM and artificial neural network (ANN)-supervised learning. Green BIM involves BIM and BPA, and these two methods have been used extensively in sustainable building design. Krygiel *et al.* first proposed the concept of Green BIM in 2008 and explained the integrated application of BIM and BPA to promote the development of sustainable design.[1] Bernstein *et al.* pointed out that Green BIM could greatly enhance the results of sustainable design through the application of BIM tools.[2]

BIM involves building information modeling and building information management. The use of BIM encompasses the entire building life cycle, including building design, construction drawing, construction, operation management, and even waste recycling. The term BIM originated from Autodesk Company's use of the concept of building information modeling in 2002 to explain the function and design of its architecture, engineering, and construction (AEC) products.[3] Nevertheless, in 1999, Eastman defined building product model concepts, technologies, and standards, which set the stage for BIM.[4] In 2008, Eastman defined BIM and related technologies in a handbook and provided BIM applications and illustrative cases for various types of participants (e.g., project owners, project managers, designers, engineers, and contractors).[5]

Although BPA and BIM consist of two different technologies, they have become increasingly integrated. BPA, which is also known as building performance simulation (BPS), involves the use of computer software to predict building performance and output visualized images, data, statistical analysis charts, and forms resulting from the simulation. BPA can help users to understand the performance of their design proposals, which will facilitate design decision-making and provide a basis for the continuing optimization of design proposals. BPA is an effective, scientific, and internationally acknowledged tool.[6] Early modeling and performance simulation tools were independent, and performance simulation tools usually consisted of two parts, where the first part was a simulation engine, which included formulas and procedures, and the second part consisted of a user interface, which facilitated the input of parameters and data and the display of results, and handled various user requirements (Fig. 2).[7] Basic building simulation work began in the 1960s and 1970s, and focused on building cooling

performance, specifically thermal load calculations and energy consumption analysis.[8,9] By the 1980s, researchers were performing analytical verification and experimental testing to improve simulation tools.[10] The focus of performance analysis shifted from energy consumption to many other building performance characteristics during the early 1990s, and integrated modeling was used to assess heat and mass transfer, airflow, and visual and acoustic performance.[11]

In recent years, BPA has gradually come to be seen as part of integrated design procedures and is generally integrated with a BIM platform. For instance, Autodesk's BIM software (Revit) includes a built-in BPA function (such as energy and lighting analysis) menu. After performing modeling with BIM software, designers can also transmit geometric and nongeometric data to simulation engines in the cloud (such as Green Building Studio), and the visualized results of analysis are transmitted back to the BIM software.[12] Although the analysis by simulation engines has required the use of third-party user interface software (such as Design Builder) for display, this role is gradually being assumed by BIM software platforms (such as Revit) (Fig. 3).

BPA is based on hypothetical models of real situations and provides approximate values. As a consequence, discrepancies inevitably exist between the results of performance simulation and the real data, which has caused the validity of the software to be extensively questioned. Nevertheless, the use of BIM models to monitor actual building operating performance during the operating management stage can provide environmental and building performance data that can be used to improve actual building management and enhance building performance.[13] If this data could be used for comparative purposes and specifically to revise the predictive values obtained during the design stage, it should be possible to improve the predictive accuracy of Green BIM.

This study recommends a supervised learning backpropagation neural network (BPN) that gains predictive capabilities through training to reduce discrepancies and uses the root mean square of error (RMSE) to confirm the results. Neural network learning roughly includes the three categories of supervised learning, unsupervised learning, and reinforcement learning. This study employed supervised learning in an attempt to reduce the data discrepancy; the

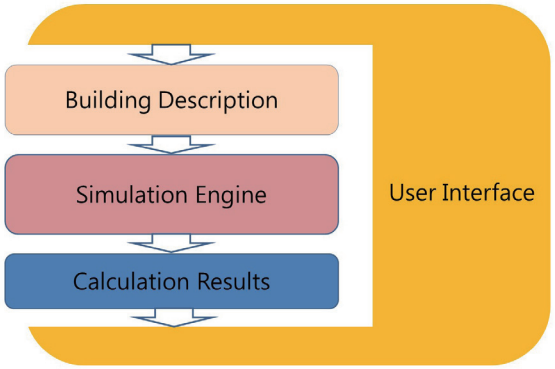

Fig. 2. (Color online) General framework of performance simulation tools.

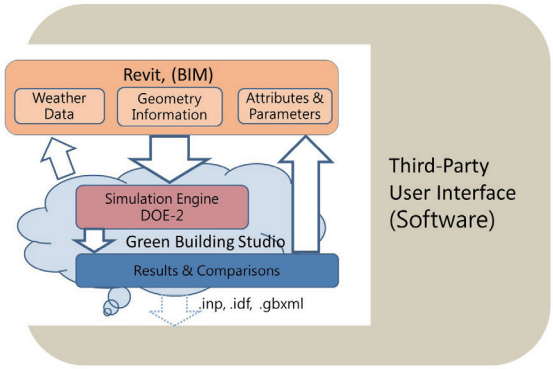

Fig. 3. (Color online) Integration of BIM and BPA technologies.

principles and theory of this process are as follows. Supervised learning is an inferential process in which the corresponding functions are derived from the inputs and outputs for given examples. For instance, the network will generate a function h approximating f from a group of examples of f. An example consists of a set $(x, f(x))$, where x is the input and $f(x)$ is the output of the function applied to x. Function h is termed the hypothesis, and the set of all possible hypotheses is termed the version space. All hypotheses in the version space must be consistent with examples. Supervised learning takes prior knowledge as the basis for a current best hypothesis search in the version space, and this consists of a search for hypothesis h best approximating the target function f. The process of searching for function f or its optimal hypothesis in a version space is known as learning or training.[14] The BPN is one of the commonly used architectures for neural network training. The output of a function can be a continuous value, called a regression analysis, or a label, called a classification. On the predictive analytics, the RMSE is usually used to evaluate the model results.[15]

The BPN has been applied to environmental performance analysis to obtain good predictive results. The method was to collect historical data from weather stations for training. Its applications included predictions of solar radiation,[16,17] air quality,[18] and wind speed.[19]

3. Theory and Method

To summarize the above literature, Green BIM emphasizes the use of BIM, a basic design tool, from the earliest stage of the design process. Responding to local climatic conditions, BPA can be used in the decision-making cycle consisting of design and analysis steps to achieve the continuing optimization of design and generate an optimized proposal consistent with environmental performance requirements. Nevertheless, when an optimized proposal derived using Green BIM is realized under real-world conditions, the simulation values obtained by the software invariably have discrepancies with the actual measured environmental performance. Taking light environment adaptation as an example, when the working surface illuminance value with a window opening ratio of X% derived by a simulation tool is Y' lux and the actually measured illuminance value in a real environment with a similar window opening ratio is Y lux, a discrepancy σ_s exists between Y' and Y (Fig. 4) [Eq. (1)].

$$\sigma_s = |Y' - Y| \tag{1}$$

In a basic BPN such as that shown in Fig. 5, data undergoes four processing stages from input to output: (1) input, (2) an aggregator function (sometimes an activation function must be added to make the aggregator function more sensitively), (3) a transfer function, and (4) output. In addition, the system estimates the cost of the actual and desired output values, calculates the error, and adjusts the weight (ω_n) in accordance with the error. The process that begins from the time the neural network starts revision until the error is less than a certain preset threshold value is termed learning, training, or adaptation. Supervised learning refers to the constant revision of the network's transmission weights to achieve consistency with the expected value. In the training process, weights are adjusted to reduce the discrepancy between the network's

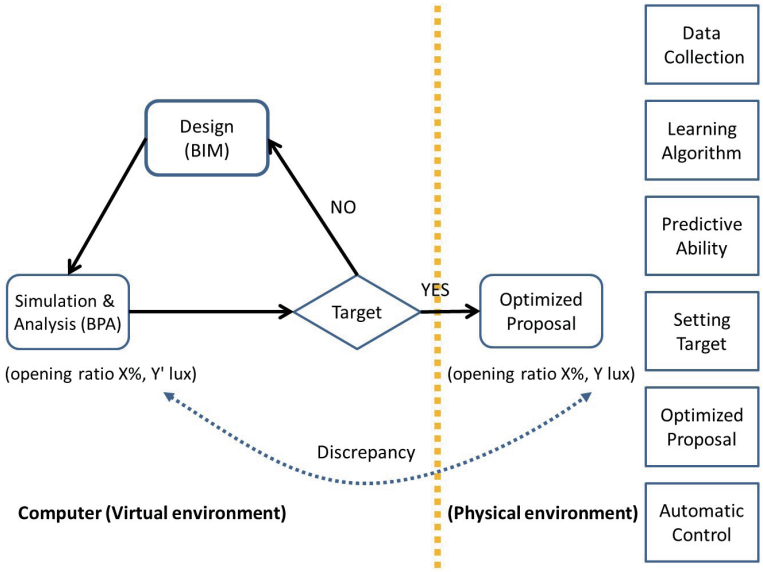

Fig. 4. (Color online) Discrepancies typically exist between simulation values and actually measured performance data in Green BIM.

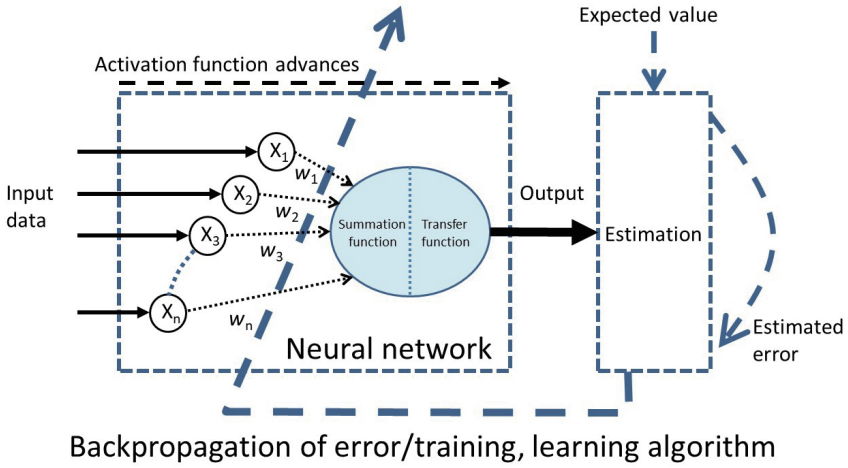

Fig. 5. (Color online) Multilayer BPN.

actual and target output values until the difference is less than a certain threshold value, at which point the process stops. In principle, a good hypothesis must generalize well, which will allow the system to make correct predictions concerning unknown examples.[20]

4. Experimental Verification

In accordance with the neural network learning characteristics and steps discussed in the previous section, this study verified the feasibility of this method in a six-step, two-stage experimental process (Figs. 6 and 7).

A. Stage 1: Data collection, learning algorithm, and acquiring predictive ability (Fig. 6). The steps are as follows:

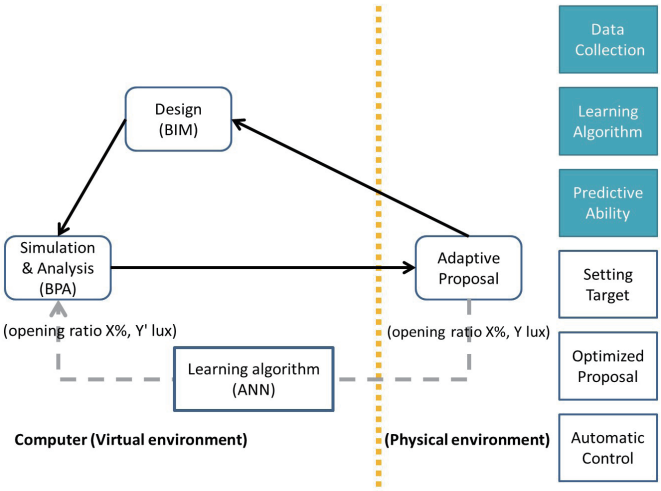

Fig. 6. (Color online) Stage 1.

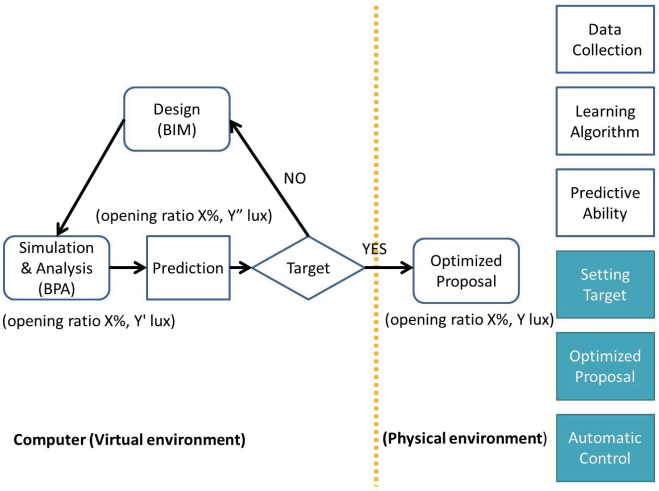

Fig. 7. (Color online) Stage 2.

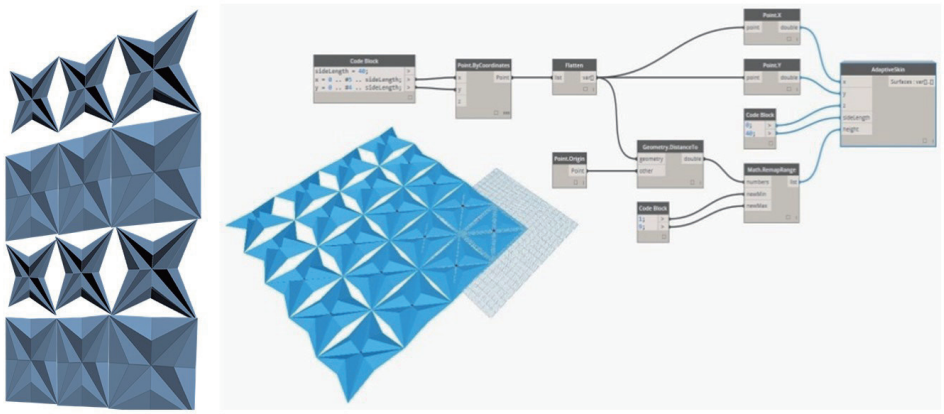

Fig. 8. (Color online) Revit modeling using Dynamo to adjust the façade window opening ratio X%.

1. BIM modeling
   Revit was used in modeling and Dynamo for consistency software was used to control the Revit model to adjust the façade window opening ratio X% (Fig. 8).
2. BPA performance simulation
   The BIM model was imported to analyze the performance of a daylight environment. The Revit model was output in gbXML format to Ecotect to simulate the working surface illuminance, and the simulated illuminance (Y' lux) was obtained from an exported text file. The latitude and longitude in this trial were (24.1638, 120.6471), and the simulation time settings consisted of three days October 1, October 9, and October 16, in 2017. The four red dots in Fig. 9 (sp_1–sp_4) represent the simulated illuminances (Y' lux) at different points in time. The recorded illuminances at the start of each hour and 30 min past each hour were used as the training set input values (Table 1), while the recorded data at 15 and 45 min past each hour were used as the testing set input values (Table 2).

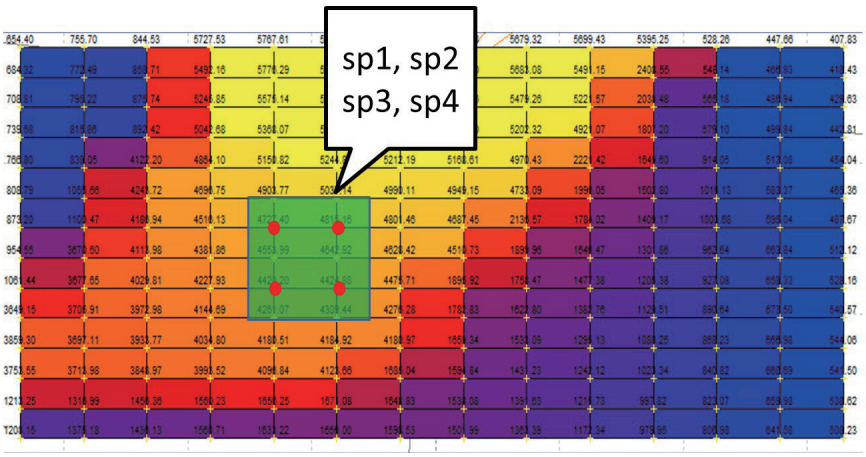

Fig. 9. (Color online) Illuminance simulation.

Table 1
Training set (excerpt).

1001 Time	sp_1	sp_2	sp_3	sp_4
7:00	3068	3166	2953	3024
7:30	4837	4968	4535	4648
8:00	6449	6642	5999	6150
8:30	7777	7913	7223	7332
9:00	8591	8720	3208	3350
9:30	3651	3742	2966	3034
10:00	3168	3322	2570	2710
10:30	2622	2711	2119	2197
11:00	2124	2276	1737	1846
11:30	1812	1884	1941	1548
12:00	1559	1659	1281	1368
12:30	1395	1450	1150	1197
13:00	1328	1426	1106	1185
13:30	1197	1285	979	1049
14:00	1124	1179	927	965
14:30	1078	1131	879	926
15:00	986	1080	804	865
15:30	875	947	704	766
16:00	705	762	574	613
16:30	522	570	427	458
17:00	323	342	260	279

Table 2
Testing set (excerpt).

1001 Time	sp_1	sp_2	sp_3	sp_4
7:15	3936	4061	3732	3853
7:45	5648	5819	5278	5399
8:15	7107	7362	6665	6758
8:45	8283	8447	7662	7750
9:15	8701	8801	3110	3211
9:45	3408	3598	2756	2907
10:15	2878	3034	2349	2490
10:45	2358	2460	1902	2015
11:15	1940	2055	1586	1682
11:45	1689	1785	1392	1484
12:15	1450	1552	1200	1282
12:45	1363	1452	1134	1212
13:15	1266	1354	1046	1118
13:45	1144	1223	936	994
14:15	1110	1159	902	936
14:45	1028	1114	848	907
15:15	930	1001	759	821
15:45	795	868	651	710
16:15	618	660	506	537
16:45	426	465	348	375

3. Actual construction and illuminance measurement

The actual construction was produced and used in accordance with the BIM model. Dynamo was linked with the plugins Firefly and Arduino, the window opening ratio (X%) was entered into Arduino to drive and control the adaptive building façade in the actual construction, and a light meter was used to measure the actual illuminance of

the working surface. The latitude and longitude at the actual structure were the same as those of the simulated location, and the actual periods consisted of the previously mentioned three days in October 2017. The four red spots (rp_1–rp_4) in Fig. 10 represent the actual measured illuminances at different points in time. The recorded illuminances at the start of each hour and 30 min past each hour were used as the training set input values (white background in Table 3), while the recorded data at 15 and 45 min past each hour were used as the testing set desired values (orange background).

4. Collection of sample data, implementation of supervised learning training, and acquisition of predictive ability

   The simulated light environment data obtained by BPA were used as the input values, and the measured illuminances from the actual structure served as the desired values. After implementing supervised learning training, the neural BPN acquired predictive ability and was able to predict the approximate Y'' (predictive values) from the Y' lux (simulation values). The following steps were employed when using neural network software to perform learning from the sample data:

   [1] This study employed NeuroSolutions software and a multilayer BPN as the learning algorithm. The training and testing sets were both selected from the sample data (Fig. 11).[21]

   [2] Definition of the input and expected values in the rows and columns of the training.

   [3] Definition of the percentage of the data set used for cross-validation: 20% in this example (Fig. 12).

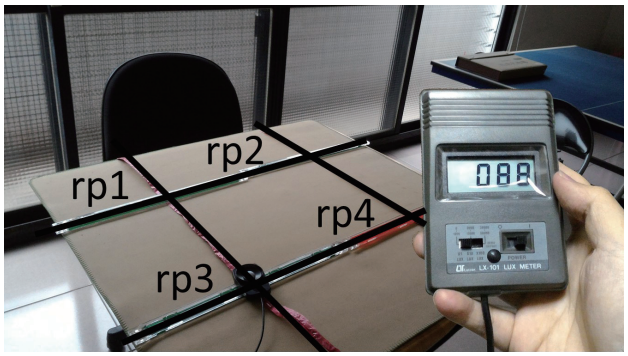

Fig. 10. (Color online) Illuminance measurement.

Table 3
Actual illuminances Y (excerpt).

Day_Time	rp_1	rp_2	rp_3	rp_4
2017/10/1_07:00	1430	1355	985	1003
2017/10/1_07:15	1816	1728	1260	1289
2017/10/1_07:30	2310	2120	1598	1580
2017/10/1_07:45	10660	8770	10920	7690
2017/10/1_08:00	15160	10020	11460	6980
2017/10/1_08:15	17150	10330	6450	5910
2017/10/1_08:30	9620	6220	2170	2220
2017/10/1_08:45	3170	2860	2020	2030
2017/10/1_09:00	2700	2650	1913	1980
2017/10/1_09:15	2480	2390	1609	1573
2017/10/1_09:30	2260	2100	1335	1525
2017/10/1_09:45	2130	2070	1425	1430
2017/10/1_10:00	2030	1990	1416	1356
2017/10/1_10:15	1890	1785	1220	1257
2017/10/1_10:30	1703	1653	1130	1156
2017/10/1_10:45	1574	1576	1096	1120
2017/10/1_11:00	1317	1294	802	869
2017/10/1_11:15	971	996	692	742
2017/10/1_11:30	805	829	578	601
2017/10/1_11:45	853	885	603	641
2017/10/1_12:00	804	815	574	627

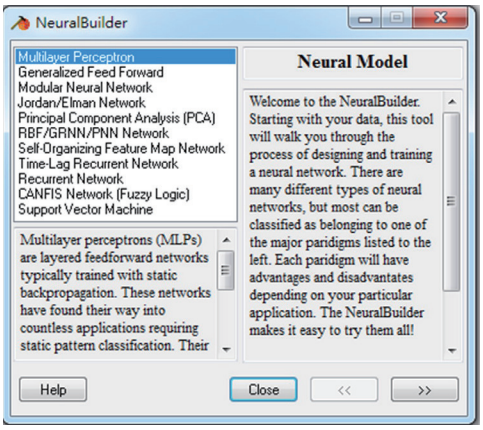

Fig. 11. (Color online) Selection of the multilayer BPN.

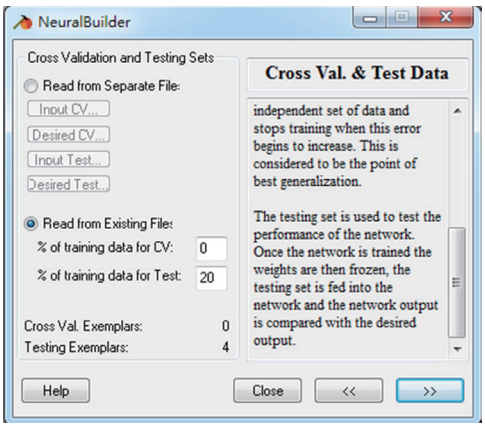

Fig. 12. (Color online) Setting of the cross-validation data set percentage.

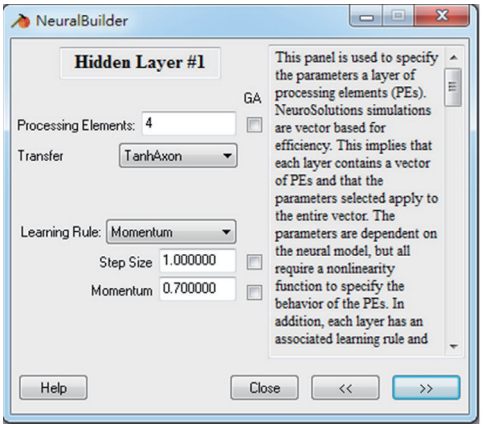

Fig. 13. (Color online) Definition of the transfer function.

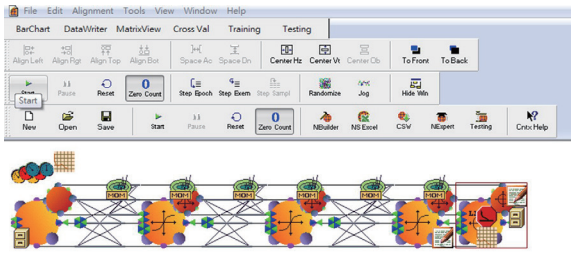

Fig. 14. (Color online) Training set learning.

[4] Definition of the transfer function: In this example, we choose the "tangent hyperbolic function" as the transfer function and adding the "momentum term" to the learning rules to increase the rate of network weight adjustment (Fig. 13).

[5] Training set learning (Fig. 14).

[6] After acquiring predictive ability, the sample data in the testing set were used to perform validation. The left side of Table 4 shows the predictive value $Y'' = ap_n$ and the right side shows the actual measured values $Y = rp_n$.

[7] It was confirmed that the network system had learned from the sample data and possessed predictive ability. As shown in Table 5, after using simulation records and on-site measurements for the three days, the simulated values sp_n were employed as the input values in the neural network training, and the measured values ap_n were taken as the expected values; the results verified that the predictive values had greater validity and good reliability, as shown below.

Table 4
Comparison of predicted values ap_n (left) and actual measured values rp_n (right) (excerpt).

ap_1	ap_2	ap_3	ap_4	Day_Time	rp_1	rp_2	rp_3	rp_4
1972	2002	1334	1390	2017/10/1_07:15	1816	1728	1260	1289
10846	7993	9073	5612	2017/10/1_07:45	10660	8770	10920	7690
12827	8509	8327	5320	2017/10/1_08:15	17150	10330	6450	5910
9469	5790	1331	1984	2017/10/1_08:45	3170	2860	2020	2030
2605	2565	1824	1770	2017/10/1_09:15	2480	2390	1609	1573
1821	1837	1240	1287	2017/10/1_09:45	2130	2070	1425	1430
1651	1650	1138	1171	2017/10/1_10:15	1890	1785	1220	1257
1396	1367	971	989	2017/10/1_10:45	1574	1576	1096	1120
1195	1144	823	838	2017/10/1_11:15	971	996	692	742
1086	1022	734	751	2017/10/1_11:45	853	885	603	641
999	922	654	677	2017/10/1_12:15	932	937	671	662
971	891	628	654	2017/10/1_12:45	1173	1140	785	797
942	857	598	627	2017/10/1_13:15	954	987	688	730
909	818	563	597	2017/10/1_13:45	961	926	597	638
898	805	551	587	2017/10/1_14:15	806	797	530	536
886	791	538	576	2017/10/1_14:45	508	522	354	341
867	769	516	557	2017/10/1_15:15	468	472	317	327
846	743	491	537	2017/10/1_15:45	923	906	672	673
823	714	462	513	2017/10/1_16:15	812	810	530	626
805	692	438	494	2017/10/1_16:45	644	623	438	460

Table 5
(Color online) Training set, test set data collection, and analysis (excerpt).

Day_Time	rp_1	rp_2	rp_3	rp_4	$\Delta(sp_1-rp_1)$	$\Delta(sp_2-rp_2)$	$\Delta(sp_3-rp_3)$	$\Delta(sp_4-rp_4)$	sp_1	sp_2	sp_3	sp_4	$\Delta(ap_1-rp_1)$	$\Delta(ap_2-rp_2)$	$\Delta(ap_3-rp_3)$	$\Delta(ap_4-rp_4)$	ap_1	ap_2	ap_3	ap_4
2017/10/1 7:00	1430	1355	985	1003					3068	3166	2953	3024								
2017/10/1 7:15	1816	1728	1260	1289	2120	2333	2472	2564	3936	4061	3732	3853	749	629	498	556	1067	1099	762	733
2017/10/1 7:30	2310	2120	1598	1580					4837	4968	4535	4648								
2017/10/1 7:45	10660	8770	10920	7690	5012	2951	5642	2291	5648	5819	5278	5399	2123	1131	902	1951	12783	9901	10018	9641
2017/10/1 8:00	15160	10020	11460	6980					6449	6642	5999	6150								
2017/10/1 8:15	17150	10330	6450	5910	10043	2968	215	848	7107	7362	6665	6758	8229	2907	3196	2750	8921	7423	3254	3160
2017/10/1 8:30	9620	6220	2170	2220					7777	7913	7223	7332								
2017/10/1 8:45	3170	2860	2020	2030	5113	5587	5642	5720	8283	8447	7662	7750	4376	3410	548	380	7546	6270	1472	1650
2017/10/1 9:00	2700	2650	1913	1980					8591	8720	3208	3350								
2017/10/1 9:15	2480	2390	1609	1573	6221	6411	1501	1638	8701	8801	3110	3211	346	249	50	112	2134	2141	1559	1461
2017/10/1 9:30	2260	2100	1335	1525					3651	3742	2966	3034								
2017/10/1 9:45	2130	2070	1425	1430	1278	1528	1331	1477	3408	3598	2756	2907	1075	997	696	727	1055	1073	729	703
2017/10/1 10:00	2030	1990	1416	1356					3168	3322	2570	2710								
2017/10/1 10:15	1890	1785	1220	1257	988	1249	1129	1233	2878	3034	2349	2490	838	715	496	559	1052	1070	724	698
2017/10/1 10:30	1703	1653	1130	1156					2622	2711	2119	2197								
2017/10/1 10:45	1574	1576	1096	1120	784	884	806	895	2358	2460	1902	2015	526	509	377	426	1048	1067	719	694
2017/10/1 11:00	1317	1294	802	869					2124	2276	1737	1846								
2017/10/1 11:15	971	996	692	742	969	1059	894	940	1940	2055	1586	1682	75	70	24	51	1046	1066	716	691
2017/10/1 11:30	805	829	578	601					1812	1884	1941	1548								
2017/10/1 11:45	853	885	603	641	836	900	789	843	1689	1785	1392	1484	191	180	111	48	1044	1065	714	689
2017/10/1 12:00	804	815	574	627					1559	1659	1281	1368								

This study uses the RMSE as the standard deviation. If the measured values are taken as the true values, then

i. the standard deviation σ_a of the predictive values ap_n and measured values rp_n at the four points was uniformly smaller than the standard deviation σ_s of the simulated values sp_n and measured values rp_n. In addition, the population standard deviation at point p_1 decreased from 2814 to 2236, that at point p_2 decreased from 2850 to 2064, that at point p_3 decreased from 2115 to 1416, and that at point p_4 fell from 2380 to 1861

(Table 6) [Eqs. (2) and (3)]. The predictive values were uniformly smaller than the simulated values at all four points and closer to the measured values, which verified that the validity of the predictive values increased after the system underwent training.

ii. The magnitudes of the decreases at points p_1 through p_4 [Eq. (4)] were 578, 786, 699, and 519, and the mean decrease was A = 645.5 [Eq. (5)]. The standard deviation σ_Δ of the decreases at the four points was 103.87 [Eq. (6)]. With regard to illuminance, the fact that the difference of 103.87 lux was not so large that the training results at the four points were reasonable and that the findings of this study had good reliability.

iii. The calculation formulas are explained as follows:

When N records are made at observation point p_n, the following formula was used to obtain the population standard deviation σ_s of the simulated values sp_n and measured values rp_n at observation point p_n:

$$\sigma_s = \sqrt{\frac{1}{N}\Sigma\left(sp_n - rp_n\right)^2}\,. \tag{2}$$

When N records are made at observation point p_n, the following formula was used to obtain the population standard deviation σ_a of the training values ap_n and measured values rp_n at observation point p_n:

$$\sigma_a = \sqrt{\frac{1}{N}\Sigma\left(ap_n - rp_n\right)^2}\,. \tag{3}$$

The formula for the magnitude of the decrease Δ between the population standard deviations σ_s and σ_a at observation point p_n was

$$\Delta = \sigma_s - \sigma_a. \tag{4}$$

When there are k observation points p, the mean A of the decrease $\Delta_{(k=1,\ldots,n)}$ from point p_1 to point p_k is obtained as

$$A = \frac{1}{n}\sum_{k=1}^{n}\Delta_k. \tag{5}$$

The standard deviation σ_Δ of the decrease from point p_1 to point p_k is obtained as

$$\sigma_\Delta = \sqrt{\frac{1}{n}\sum_{k=1}^{n}\left(\Delta_k - A\right)^2}\,. \tag{6}$$

Table 6
Changes in standard deviation from p_1 to p_4 (from $RMSsp_n$ to $RMSap_n$).

$RMSsp_1$	$RMSsp_2$	$RMSsp_3$	$RMSsp_4$	$RMSap_1$	$RMSap_2$	$RMSap_3$	$RMSap_4$
2814	2850	2115	2380	2236	2064	1416	1861

B. Stage 2: Setting of targets in accordance with prediction, finding an optimized adaptation plan, and performing automated control (Fig. 7). The following steps were employed:

5. Finding an optimized adaptation plan

   After the system acquired predictive ability, it was able to use the predictive value Y'' as its target setting condition and find an optimized adaptation plan. In other words, in the future, it will only be necessary to input a simulation value set as the testing set in the trained neural network, and the network will be able to obtain the corresponding predictive values. Regarding the setting of targets, taking the light environment as an example, illuminance levels can be set according to the planned uses and activities of a space referring to Chinese National Standards (CNS) illuminance standards. For instance, the function of the location of the actual measurements was designated as a studio, which had the uses of reading and writing. As a result, the appropriate illuminance scope for working surfaces within the space was set as 500–1000 lux (Table 7). The window opening ratio X% and predictive value Y in the adaptation plan had to satisfy this target setting range.

6. Implementation of script-oriented automatic control

   In accordance with the parameters of the optimized proposal, Dynamo relied on linkage with the Firefly and Arduino plugins to perform script-oriented automatic control to drive the adaptive façade elements of the actual structure. This system operated in a cyclic fashion and enhanced environmental quality by responding to environmental changes by employing adaptive mechanisms. The figure below shows how Dynamo sends and receives data from the Arduino software IED via the plugin Firefly to control the embedded microprocessor and execute the script to the operator to trigger device actions (Fig. 15).[23]

Table 7
CNS indoor illuminance standards (excerpt).[22]

Illuminance (lux)	Living room	Studio	Children's room
1000–2000	○Handicrafts		
750–1000	○Sewing	○Writing ○Reading	○Homework ○Reading
500–750	○Reading ○Makeup ○Telephone use		

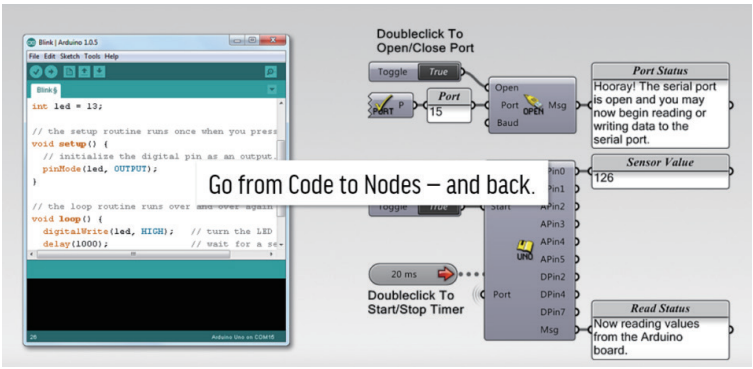

Fig. 15. (Color online) Firefly plug-in driving Arduino IED.[23]

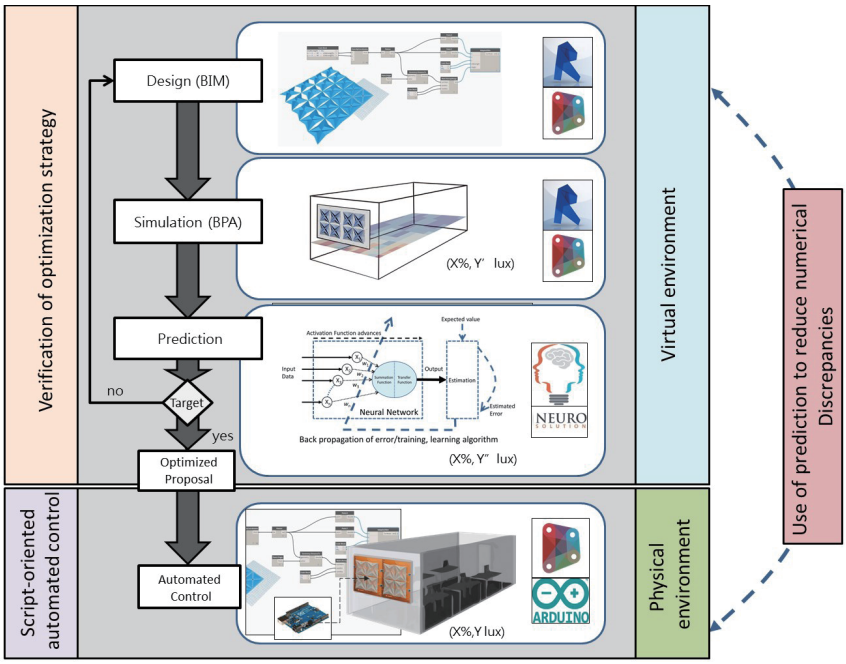

Fig. 16. (Color online) Completed building prediction and control system.

5. Conclusions and Recommendations

BPS simulation values are approximations of real values. The greater the validity of Green BIM, the better it can discover problems early in the design stage, enabling the proposal of precise decision-making strategies and marked reductions in construction and operating costs. ANN-supervised learning can reduce the discrepancy between predictive and actual values and enhance the validity of Green BIM. In accordance with the theory and method outlined in this paper, a six-step, two-stage process was employed to verify the optimization strategy in a virtual environment, construct an adaptive mechanism based on the light environment in a physical environment, and perform script-oriented automated control. The completed building prediction and control system was compiled as shown in Fig. 16. This system enables design and analysis work during the initial stage of Green BIM to be used in conjunction with environmental data during the operating management stage, which can boost the validity of Green BIM through the use of environmental data records and feedback. In addition, recommendations for further research are as follows:

(1) The standard deviation in Eqs. (2) and (3) is also known as the mean Euclidean distance (MED) and is an indicator of the distance between the prediction and learning sample points of a neural network.[24] The smaller the MED value, the closer the predicted time sequence values are to the true values. Although this study has shown that the validity of the predictive values increased, whether an algorithm to find the minimum sampling distance exists must await future research.

(2) BPA is gradually being considered as part of integrated design procedures and is increasingly integrated with BIM platforms. The BIM platform Revit can already use a lighting analysis

plugin to analyze natural lighting and visualize illuminance. However, this plugin lacks a numerical output function. The Ecotect software used in this study was withdrawn from update service in March 2015, and illuminance analysis can only be performed by exporting data from the Revit model in gbXML format to Ecotect, which cannot be considered a fully integrated part of the BIM platform. In the future, if lighting analysis plugins can add a numerical output function, this will facilitate the convenient generation of predictive values and enable script-oriented automatic control. In this way, the integrated light environment adaptive capability of Green BIM will become increasingly accurate and effective.

(3) This study takes daylight simulation as an example, but its method can also be applied to climate analysis, thermal comfort, energy calculations, and other BPA dimensions.

Acknowledgments

This work was supported by MOST 104-2221-E-035-066 Green-BIM-based energy conservation and carbon reduction design optimization decision-making applications, and the Ministry of the Interior Architecture & Building Research Institute project "Taiwan green building information modeling application framework research".

References

1 E. Krygiel, B. Nies, and S. McDowell: Green BIM-Successful Sustainable Design with Building Information Modeling (Wiley, 2008) pp. 178–195, 215–218.
2 H. M. Bernstein, M. A. Russo, and S. A. Jones, Eds.: Smart Market Report: Green BIM: How Building Information Modeling is Contributing to Green Design and Construction (McGraw-Hill Construction, 2010) pp. 4–6.
3 Autodesk: Building Information Modeling (Autodesk, Inc., 2002). http://www.laiserin.com/features/bim/autodesk_bim.pdf (accessed January 2019).
4 C. M. Eastman: Building Product Models (CRC, 1999). http://doi.org/10.1201/9781315138671
5 C. M. Eastman: BIM Handbook: a Guide to Building Information Modeling for Owners, Managers, Designers, Engineers, and Contractors (Wiley, 2008). https://doi.org/10.5130/AJCEB.v12i3.2749
6 A. Shandy, L. M. J. Hensen, L. Beltrán, and A. D. Herde: J. Build. Perform. Simul. **5** (2012) 155. https://doi.org/10.1080/19401493.2010.549573
7 T. Maile, M. Fischer, and V. Bazjanac: Building Energy Performance Simulation Tools - a Life-Cycle and Interoperable Perspective (Stanford University, 2007). http://automatica.dei.unipd.it/public/Schenato/PSC/2010_2011/gruppo4-Building_termo_identification/IdentificazioneTermodinamica20072008/Biblio/Articoli/Standorf%20Univ%20Performance%20Buildings.pdf (accessed January 2019).
8 T. Kusuda: Early History and Future Prospects of Buildings System Simulation (IBPSA, 1999). http://www.ibpsa.org/%5Cproceedings%5CBS1999%5CBS99_P-01.pdf (accessed January 2019).
9 J. A. Clarke: Energy Simulation in Building Design (Science Direct, 2001) 2nd ed. https://doi.org/10.1016/B978-075065082-3/50003-6
10 G. Augenbroe: Build. Environ. **37** (2002) 189. https://doi.org/10.1016/S0360-1323(02)00041-0
11 G. Augenbroe: Build. Environ. **27** (1992) 149. https://doi.org/10.1016/0360-1323(92)90019-L
12 Emilekfouri: Advanced Energy Analysis with Green Building Studio DOE2 and EnergyPlus Support (Autodesk Green Building Studio, 2013). http://blogs.autodesk.com/insight360/advanced-energy-analysis-with-green-building-studio-doe2-and-energyplus-support/ (accessed January 2019).
13 P. Teicholz, Ed.: BIM Guide for Facility Managers (Wiley, 2013) pp. 41–42, 53.
14 S. Haykin: Neural Networks: A Comprehensive Foundation (Prentice Hall, 1999) 2nd ed. https://doi.org/10.1016/0925-2312(95)90026-8
15 B. Widrow and M.A. Lehr: Proc. IEEE **78** (1990) 1415. https://doi.org/10.1109/5.58323
16 A. S. S. Dorvlo, J. A. Jervase, and A. Al-Lawati, Appl. Energy **71** (2002) 307. https://doi.org/10.1016/S0306-2619(02)00016-8

17 A. K. Yadav and S. S. Chandel: Renewable Sustainable Energy Rev. **33** (2014) 772. https://doi.org/10.1016/j.rser.2013.08.055
18 M. Kolehmainen, H. Martikainen, and J. Ruuskanen: Atmos. Environ. **35** (2001) 815. https://doi.org/10.1016/S1352-2310(00)00385-X
19 R. Velo, P. López, and F. Maseda: Energy Convers. Manage. **81** (2014) 1. https://doi.org/10.1016/j.enconman.2014.02.017
20 J. C. Principe, N. R. Euliano, and W. C. Lefebvre: Neural and Adaptive Systems: Fundamentals Through Simulations (Wiley, 2000) pp. 1–24, 150.
21 NeuroSolutions (2016). http://www.neurosolutions.com/ (accessed January 2019).
22 CNS Indoor Illuminance Standard (2016): http://www.homewell.tw/classroom/evn-class/e05-02.htm (accessed January 2019).
23 Firefly (2016): http://www.fireflyexperiments.com/#home (accessed January 2019).
24 J. C. Yu, X. Chen, T. R. Hung, and F. Thibault: J. Intell. Manuf. **15** (2004). https://doi.org/10.1023/B:JIMS.0000037712.33636.41

About the Author

Shang Yuan Chen received his M.S. degree from Yale University, USA, in 2000 and his Ph.D. degree from National Cheng Kung University, Taiwan, ROC, in 2007. From 2008 to 2012, he was an assistant professor at Feng Chia University, Taiwan, ROC. Since 2012, he has been an associate professor at the School of Architecture and Vice Director of BIM Research Center, Feng Chia University. His research interests are in intelligent architecture and building information modeling. He has published 29 journal papers (including in EI, SCI, SSCI, and AHCI), 71 conference papers, and one book, been awarded 20 patents, presided over 20 Ministry of Science and Technology projects, and twice won Outstanding Scholar Awards from the Ministry of Science and Technology.